PAPER

Check for updates

Formation of plasmonic core/shell nanorods through ammonia-mediated dissolution of silver(I) oxide for ammonia monitoring

Elahe Ghorbanian,[a] Forough Ghasemi, [ID] *[b] Kamran Rezaei Tavabe[a] and Hamid Reza Alizadeh Sabet[c]

Due to the expansion of the aquaculture industry in the world and the importance of controlling ammonia in fish breeding water, high levels of which impose significant damage to fish farming, it is crucial to develop affordable, rapid, and on-site methods for timely and accurate detection of ammonia. In this study, a colorimetric sensor based on the formation of gold/silver core/shell nanorods (NRs) was developed for the rapid detection of ammonia. The sensor functioned by the specific dissolution of silver(I) oxide by ammonia, which triggered the activation of silver ions and the subsequent formation of gold/silver core/shell NRs in the presence of a reducing agent (*i.e.*, ascorbic acid (AA)). This led to changes in the surface composition, size, and aspect ratio of the NRs, which was accompanied by a vivid color change from green to red/orange in less than a minute. The colorimetric sensor was optimized by adjusting the effective parameters, including ascorbic acid, silver ion, and sodium hydroxide concentration as well as pH and reaction time. After the optimization process, the sensor was found to have a linear range from 50 to 800 μmol L^{-1} (0.85–13.6 ppm). In addition, the application of the sensor was validated by measuring the ammonia content in water samples from rearing ponds for rainbow trout, sturgeon, and tilapia before and after feeding. The sensor's label-free, rapid, user-friendly, naked-eye, and cost-effective operation makes it an attractive option for on-site environmental monitoring of ammonia.

1. Introduction

Ammonia is a common substance used in various industries, *e.g.* in chemical fertilizers, cooling systems, in the manufacture of paints, in medicine, and in explosives. Exposure to this substance poses serious health risks and is harmful to humans and animals, especially aquatic life.[1] Aquaculture involves the cultivation of aquatic organisms under controlled or semi-controlled conditions.[2] To ensure sustainable aquaculture, it is essential to maintain the quality of the water and inputs, promote fish health, select pollution-free sites, and strictly control water quality parameters. Water quality, including carbon dioxide levels, salinity, oxygen levels, temperature, and the presence of pollutants such as ammonia, can significantly affect the response of aquatic animals to stress and their overall health.[3]

Ammonia is a pollutant that is frequently found in aquatic ecosystems. In closed aquaculture systems, however, the accumulation of ammonia is a critical challenge. This is all the more true as ammonia levels tend to rise due to the accumulation of fish waste and the decomposition of excess feed.[4] This compound occurs in nature, but is also introduced by sewage, industrial waste, and agricultural runoff.[5] Even low concentrations of dissolved ammonia can have a negative effect on aquatic life, as it is a harmful chemical compound. Ammonia is the most important toxic pollutant in fish tank wastewater.[6] In fish, ammonia can lead to physical damage, behavioral changes, and even death.[7] The tolerance of fish species to ammonia varies according to their physiological status.[8] Maintaining adequate water quality in aquaculture is therefore crucial, and controlling ammonia concentrations is particularly important. However, measuring the ammonia content can be difficult and expensive. It requires specialized equipment and trained professionals, which can be a major hurdle for many aquaculture producers.

A number of techniques have been developed to regulate and monitor ammonia concentrations, including the Nessler and Indophenol Blue (IPB) methods. However, for reasons of environmental protection and the need to detect low concentrations, these methods are not recommended.[9] The indophenol blue method is based on the indophenol or Berthelot reaction.[4]
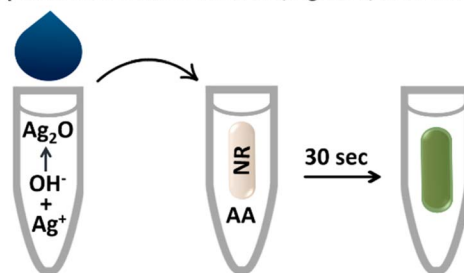
[a]Department of Fisheries, Faculty of Natural Resources, University of Tehran, Karaj, Iran

[b]Department of Nanotechnology, Agricultural Biotechnology Research Institute of Iran (ABRII), Agricultural Research, Education, and Extension Organization (AREEO), Karaj, Iran. E-mail: forough.ghasemi@abrii.ac.ir

[c]International Sturgeon Research Institute, Iranian Fisheries Science Research Institute, Agricultural Research, Education, and Extension Organization (AREEO), Rasht, Iran

Nessler's method uses mercury, which must be disposed of as hazardous waste. The ammonium salicylate test method is more expensive and slower. This test generates sodium nitroferricyanide and must be disposed of as hazardous waste. Ammonia can also be measured with ion electrodes. With this method, it is important to know the water temperature, pH and salinity in order to evaluate the results of ammonia.[7] Furthermore, the purchase of these devices involves additional costs, *e.g.* for calibration solutions, cables, and additional sensors, which makes them costly and impractical for small aquaculture producers. In addition, delays in testing can lead to fluctuations in ammonia levels and thus affect the test results.[4] As it is important to detect low levels of ammonia quickly, it is essential to develop methods that are both efficient and easy to use. In this research, a fast, simple, and inexpensive colorimetric method without hazardous waste disposal was developed using plasmonic nanorods to measure ammonia.

Plasmonic nanostructures of gold and silver are considered as efficient sensing elements due to their unique photophysical properties, size-dependent optical changes, simplicity, and high sensitivity in colorimetric measurement of various chemical species.[10–12] One of the most important and widely used properties of plasmonic nanoparticles is their surface plasmon resonance (SPR) phenomenon. The reason for this phenomenon is the combined oscillation of conduction electrons on the metal surface, which is triggered by exposure to light and leads to intense absorption in the visible electromagnetic spectrum. As a result, the solution of nanoparticles appears in a vivid color.[13,14] The surface plasmon resonance leads to extremely high absorption and scattering properties in the visible wavelength range, which gives the particles a higher sensitivity than conventional organic dyes and makes them suitable for use as colorimetric sensors.[15–22]

In this study, gold nanorods (AuNRs) were used, which exhibit two distinct surface plasmon resonance peaks: the transverse peak at approximately 520 nm and the longitudinal peak, which varies from the visible to the near-infrared absorption range depending on the aspect ratio (AR) of the AuNRs. As the AR decreases, the longitudinal peak of the SPR shifts to shorter wavelengths, resulting in a blue shift and a vivid color change. Therefore, AuNRs are very promising for applications as signal transducers in the development of sensors and biosensors.[23–26] In general, AuNRs are used in sensor design based on various mechanisms, including etching and formation/growth.[27] In growth-based methods, the analyte directly or indirectly reduces metal ions and forms core/shell nanoparticles.[28] In the present study, we have utilized the growth mechanism and the design of the sensor is based on the specific dissolution of silver(I) oxide by ammonia, which triggers the activation of silver ions and the subsequent formation of core/shell gold/silver nanorods in the presence of ascorbic acid (AA) as a reducing agent (Scheme 1). This leads to changes in the surface composition, size and aspect ratio of the AuNRs in the plasmonic ribbon, which are accompanied by vivid color changes in the solution. As far as we know, there are no previous reports of a nanosensor for rapid detection of ammonia in multiple colors.
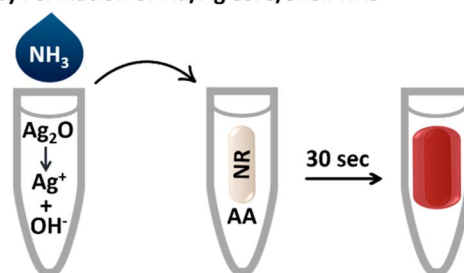
Scheme 1 Rapid and visual monitoring of ammonia in (a) ammonia-free sample and (b) ammonia-containing sample. Silver ions (Ag^+) can be reduced by ascorbic acid (AA) to produce Au/Ag core/shell NRs. In the presence of hydroxide ions, silver ions form silver(I) oxide, and as a result, restrain/reduce the silver deposition on the surface of AuNRs. In ammonia-containing samples, silver(I) oxide is specifically dissolved by ammonia and is deposited on the surface of AuNRs to form Au/Ag core/shell AuNRs.

2. Experimental section

2.1. Materials

The reagents and chemicals used in this study include chloroauric acid ($HAuCl_4$), silver nitrate ($AgNO_3$), sodium borohydride ($NaBH_4$), sodium hydroxide ($NaOH$), cetyl-trimethylammonium bromide (CTAB), ascorbic acid (AA), sodium carbonate (Na_2CO_3), 5-bromosalicylic acid (5-BrSA), sodium bicarbonate ($NaHCO_3$), ascorbic acid ($C_6H_8O_6$) and ammonia (NH_3) were procured from Sigma and were of analytical grade. Deionized water (DI) was used for all steps of this study.

2.2. Instrumentation

The UV-Vis spectrophotometer (PerkinElmer) with a 0.1 cm cuvette was used to record the absorption spectra in the 380–900 nm range. A Wisestire stirrer (model MSH-20D) was used for the experiments. pH measurements were performed with a Denver pH meter (model 270) equipped with a Metrohm glass electrode. The size of the nanoparticles was investigated using a TEM Philips EM 208S, with an accelerating voltage of 100 kV and a maximum resolution of less than 0.2 nm. Germany KERN & Sohn GmbH, model ABJ220-4M, with an accuracy of 4 decimal places was used for the weight measurements. The required volumes of the solutions (less than 1.0 mL) were taken with samplers from Eppendorf, Germany. The digital images were taken with a 12 megapixel camera (iPhone 13).
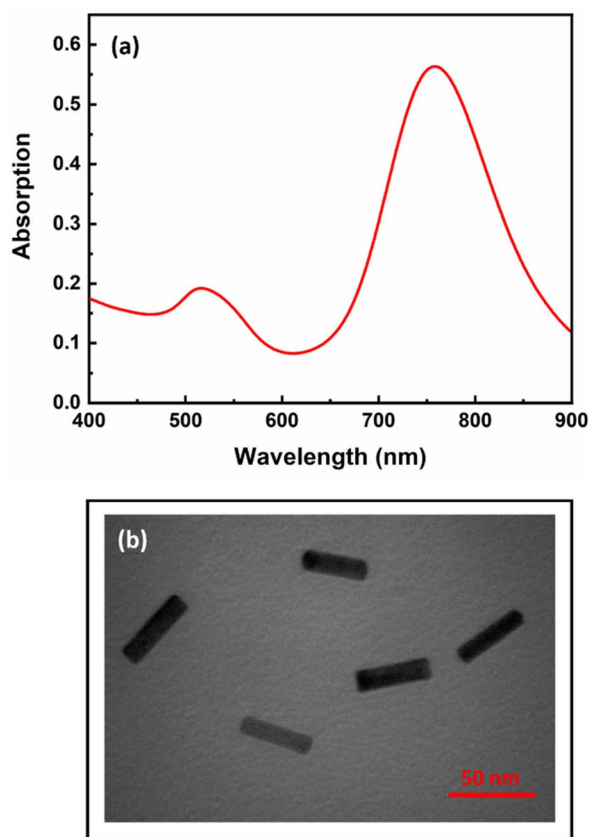
Fig. 1 (a) UV-Vis spectrum and (b) TEM image of the synthesized AuNRs.

2.3. Synthesis of AuNRs

In order to synthesize rod-shaped gold nanoparticles (AuNRs), a solution of primary seeds was first prepared.[29] To prepare the seed solution, 0.125 mL of a 0.01 mol L^{-1} HAuCl$_4$ solution was added to 4.7 mL of a 0.1 mol L^{-1} CTAB solution under magnetic stirring, followed by the addition of 0.3 mL of a 0.01 mol L^{-1} NaBH$_4$ solution. After mixing, the yellow-brown solution was allowed to stand at room temperature for two hours before use.

To prepare AuNRs, 10 mg of 5-BrSA was added to a 5.0 mL solution of CTAB (0.1 mol L^{-1}). After complete dissolution, a volume of 96 μL of a 0.01 mol L^{-1} AgNO$_3$ solution was added. After 15 minutes of gentle stirring at room temperature, 5.0 mL of a HAuCl$_4$ solution (0.001 mol L^{-1}) was added. After 50 minutes, 26 μL of a solution containing 0.1 mol L^{-1} AA was added to the mixture and stirred vigorously for 1 minute. Finally, 16 μL of the primary seed solution was injected into the above solution and stirred for 30 s. Then, it was allowed to stand undisturbed at room temperature for 12 hours. A brown hue gradually developed in the solution and AuNRs with transverse and longitudinal peaks at 522 and 728 nm, respectively were synthesized.[29]

2.4. Sensing procedure

AA solution with a final concentration of 3.0 mmol L^{-1} was added to 200 μL AuNRs solution and made uniform and homogeneous by pipetting. Silver nitrate, NaOH, and carbonate buffer (pH = 9.6) with a final concentration of 260 μmol L^{-1}, 2.5 mmoL^{-1}, and 10 mmol L^{-1}, respectively, were added to another microtube and made uniform and homogeneous by pipetting. Then DI water (as blank) or ammonia solution was added to this microtube. Finally, the contents of this microtube were slowly added to the first microtube (the final volume was 1.0 mL) and pipetted for 30 seconds. The absorbance spectra were measured with a UV-Vis spectrophotometer and the color of the solutions was recorded with a cell phone camera.
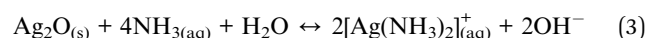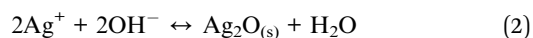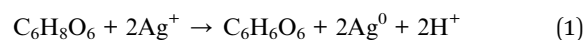
2.5. Assessment of matrix effect

A 25 mmol L^{-1} solution of NaCl, NaNO$_3$, NaNO$_2$, Na$_2$HPO$_4$, FeCl$_3$·6H$_2$O, CuCl$_2$, Na$_2$SO$_4$, ZnCl$_2$, AlCl$_3$·6H$_2$O, CaCl$_2$, KCl, Na$_2$CO$_3$, MgCl$_2$, CoCl$_2$, CrCl$_3$, HgCl$_2$ was prepared. To check the influence of these ions on the reaction of the probe, all steps were carried out with the same procedure explained in Section 2.4. With the difference that an ion solution was added to the probe instead of the ammonia solution.

In the next step, the performance of the sensor was evaluated in real samples, including water from the campus and tap water, as well as water samples from rainbow trout, sturgeon, and tilapia rearing ponds. The water from the sturgeon pond and the inlet was taken from the ponds of the International Sturgeon Research Institute, Rasht, Iran. The water for tilapia and trout farming was taken from the Fisheries Workshop of the Faculty of Agriculture and Natural Resources of Tehran University in Karaj, Iran. All samples were used immediately after passing through filter paper.

3. Results and discussion

3.1. Design principle

The synthesized AuNRs with an aspect ratio of 3.6 (length/width: 43 nm/12 nm) exhibited two transverse and longitudinal SPR peaks at 521 and 760 nm, respectively (Fig. 1). Ascorbic acid (AA, C$_6$H$_8$O$_6$) has the ability to reduce silver ions (eqn (1)). In the presence of AuNRs, the AuNR acts as a nucleus and the silver ions are reduced and deposited on its surface, forming a silver shell.[28] The formation of Au/Ag core/shell NRs led to changes in the surface composition, size and aspect ratio of the AuNRs, which consequently altered their plasmonic band (Fig. 2a, B: red line). These changes were also observed as significant variations in the color of the sensor solution.

$$C_6H_8O_6 + 2Ag^+ \rightarrow C_6H_6O_6 + 2Ag^0 + 2H^+ \quad (1)$$

$$2Ag^+ + 2OH^- \leftrightarrow Ag_2O_{(s)} + H_2O \quad (2)$$

$$Ag_2O_{(s)} + 4NH_{3(aq)} + H_2O \leftrightarrow 2[Ag(NH_3)_2]^+_{(aq)} + 2OH^- \quad (3)$$

By adding sodium hydroxide to the silver ions, the silver ions form silver(I) oxide (Ag$_2$O) (eqn (2)), which inhibits the formation of a silver shell on the surface of the AuNRs (Fig. 2a, C: blue line). It should be noted that in the same condition of the sensor, the inhibitory effect of other anions such as phosphate, sulfate, chloride, and bromide was also investigated and none
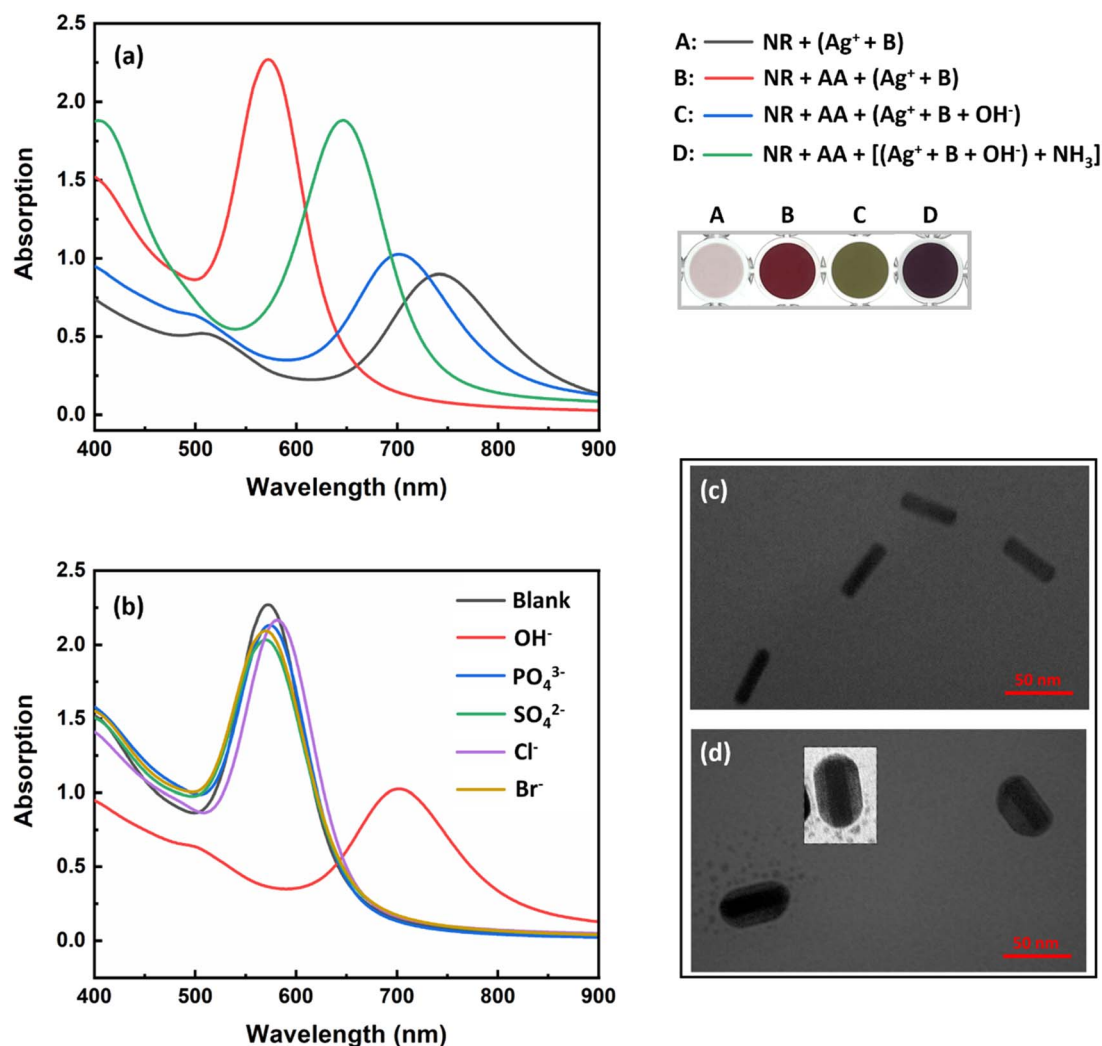
Fig. 2 (a) UV-Vis spectra and color of AuNRs in the presence of silver ions and buffer (A: black line); ascorbic acid, silver ions, and buffer (B: red line); ascorbic acid, silver ions, buffer, and sodium hydroxide (C: blue line); ascorbic acid, silver ions, buffer, sodium hydroxide, and ammonia (D: green line). Photos were taken from the top of a 96-well microplate. (b) UV-Vis spectra of AuNRs in the presence of ascorbic acid, silver ions, buffer, and anions. TEM images of the sensor containing ascorbic acid, silver ions, buffer, and sodium hydroxide (c) before and (d) after the addition of ammonia. The concentration of ascorbic acid, silver ions, buffer, ammonia, and anions was 2.4 mmol L^{-1}, 220 μmol L^{-1}, 10 mmol L^{-1} (pH 9.5), 2.0 mmol L^{-1}, 10 mmol L^{-1}, respectively.

of them inhibited the activity of silver ions. As Fig. 2b shows, core/shell NRs were prepared in the presence of all anions except hydroxide.

The presence of ammonia specifically caused the dissolution of silver(I) oxide and the activation of silver ions (eqn (3) and Fig. 2a, D: green line). It is worth noting that this part of the chemistry behind the design principle was based on the well-known Tollens' reagent, in which only ammonia can dissolve silver oxide. Therefore, in the presence of ammonia, gold/silver core/shell AuNRs were formed and a vivid color and spectral change was observed in the probe (Scheme 1 and Fig. 2a). The formation of the core–shell nanorods was confirmed by acquiring TEM images before and after the addition of ammonia to the sensor (Fig. 2c and d). In the presence of ammonia, a decrease in the aspect ratio of the AuNRs from 3.6 to 2.8 was observed, indicating the deposition of a silver layer on the surface of the AuNRs.

Following the satisfactory initial results, various parameters affecting the sensor's response to ammonia were optimized to achieve the highest sensitivity of the sensor. In all experiments, the maximum wavelength difference between the blank and the ammonia sample ($\lambda_0 - \lambda$) was used as the response of the sensor.

3.2. Optimization of effective parameters

The optimum condition for maximum sensitivity of the sensor was achieved by fine-tuning various parameters such as ascorbic acid concentration, silver ion concentration, hydroxide ion concentration, pH and time. To produce core/shell gold/silver NRs, ascorbic acid was used as a weak reducing agent being able to reduce silver ions (Ag$^+$) to silver atoms (Ag^0) on the surface of gold nanorods (eqn (1)). At the beginning of the study, a range of ascorbic acid concentrations between 0.25 and 4.5 mmol L^{-1} was investigated. As can be seen in Fig. 3a, the
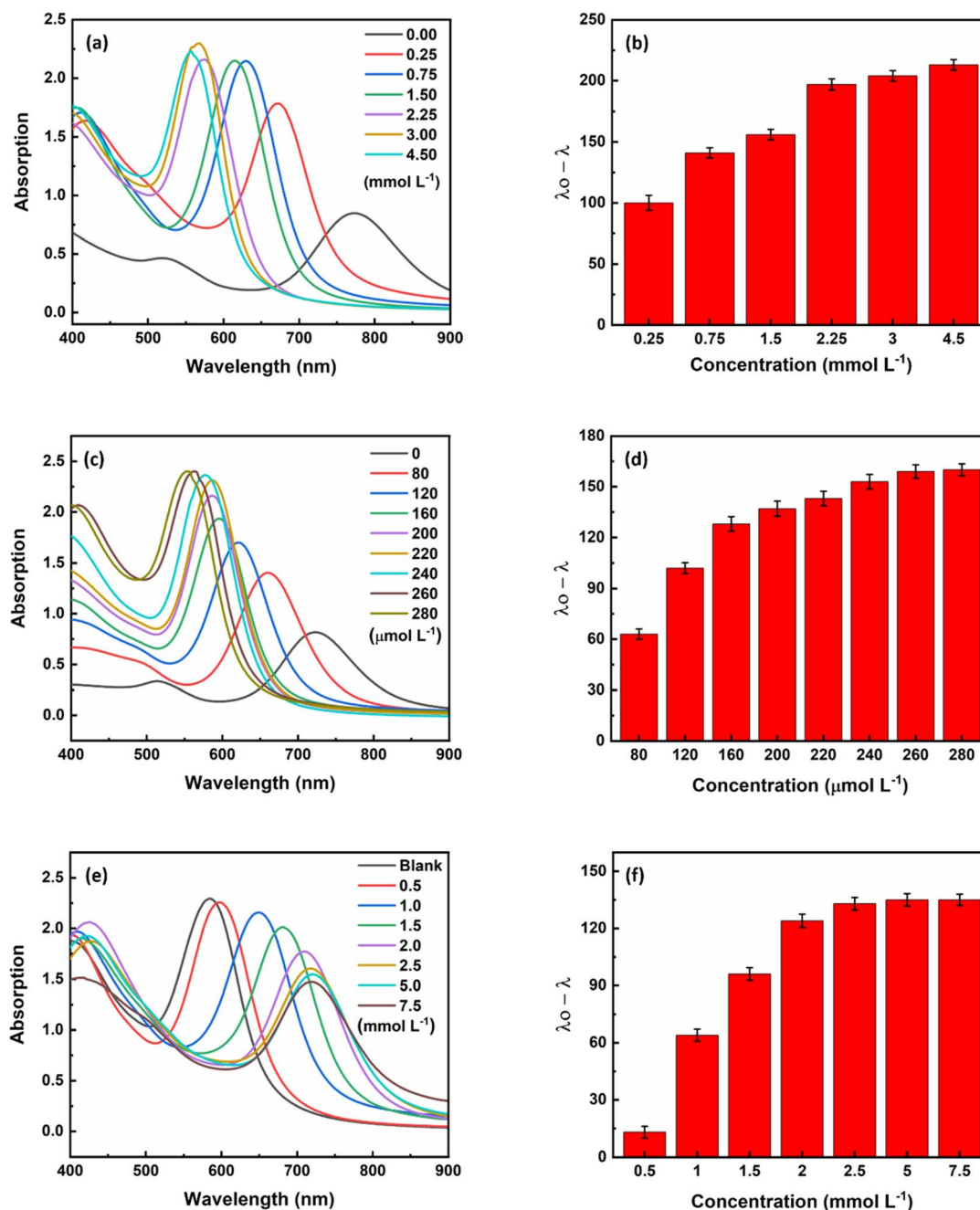
Fig. 3 UV-Vis spectra and corresponding bar plots illustrating the effect of (a and b) ascorbic acid, (c and d) silver ions, and (e and f) sodium hydroxide concentration on the formation of gold/silver core/shell NRs.

longitudinal plasmon peak of the nanorods shifted to shorter wavelengths with increasing ascorbic acid concentration. This is because the silver reduction increases with increasing ascorbic acid concentration (eqn (1)), leading to the formation of core/shell nanorods with a lower aspect ratio. After analyzing different concentrations of ascorbic acid (Fig. 3b), it was found that the signal reached a plateau at 3.0 mmol L^{-1} and was therefore chosen as the optimum concentration for the subsequent experiments.

In the next step, the concentration of coating material, *i.e.*, silver ions was optimized as a crusial parameter. With an increase in the silver ion concentration, which can be attributed to an increase in the thickness of the silver layer, a corresponding increase in the blue shift of the plasmon peak was observed (Fig. 3c). At a silver ion concentration of 260 μmol L^{-1}, the magnitude of the plasmon peak shift was fixed (Fig. 3d), so the concentration of 260 μmol L^{-1} silver ions was chosen as the optimal concentration for further experiments.

In the presence of sodium hydroxide, silver(I) oxide (Ag$_2$O) is formed (eqn (2)), which inhibits the formation of a silver shell on the surface of the AuNRs. Therefore, the concentration of hydroxide ions was optimized as an inhibitor for the formation
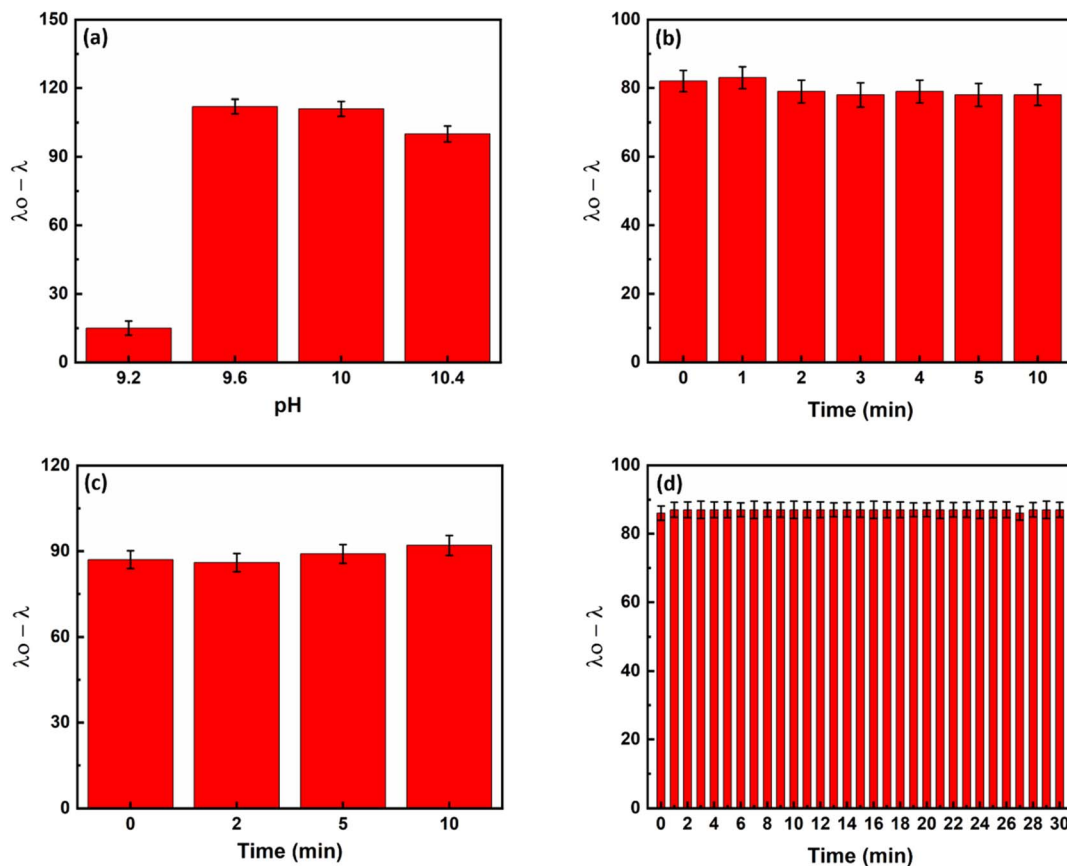
Fig. 4 The effect of (a) pH, (b) inhibition time, (c) recovery time, and (d) analysis time on the sensor's response. The concentration of ascorbic acid, silver ions, buffer, sodium hydroxide, and ammonia was 3.0 mmol L^{-1}, 260 µmol L^{-1}, 10 mmol L^{-1}, 2.5 mmol L^{-1}, and 2.0 mmol L^{-1}, respectively.

of gold/silver core/shell NRs. As shown in Fig. 3e, as the hydroxide ion concentration increased, the amount of core–shell nanoparticles formed decreased until the inhibition was as high as possible at a concentration of 2.5 mmol L^{-1} (Fig. 3f). Therefore, the concentration of 2.5 mmol L^{-1} sodium hydroxide was chosen as the optimum concentration.

As eqn (1) illustrates, reducing silver ions and consequently forming core/shell NRs is pH-dependent. Initial experiments revealed that the rate of silver metallization is low at pH values below 7.0. Therefore, the experiments were done at basic pHs. Among different tested buffers, the carbonate–bicarbonate buffer had no interferences with the responses. Carbonate–bicarbonate buffer is an effective buffer in the range of 9.2–10.6. Therefore, pH was investigated in this range using the carbonate–bicarbonate buffer. According to Fig. 4a, the highest response of the sensor was observed at a pH of 9.6 and remained constant thereafter. Therefore, all subsequent experiments were carried out at a pH value of 9.6.

To achieve the maximum response in the shortest possible time, we tested three times, including inhibition, recovery and analysis times, which could affect the response of the sensor. By combining hydroxide and silver ions and recording the response of the sensor at different times, the inhibition time was investigated. Based on the results shown in Fig. 4b, the

reaction between hydroxide and silver ions to form silver(ı) oxide was already completed by mixing. Therefore, we used the mixture of hydroxide ions and silver ions immediately after mixing.

The recovery time was then optimized. For this purpose, ammonia was added to the deactivated silver solution (the mixture of silver and hydroxide). As can be seen in Fig. 4c, ammonia dissolves the silver oxide in the first few seconds and thus reactivates the silver ions. Therefore, the mixture of ammonia and silver oxide was used as soon as it was completely mixed.

Finally, the analysis time was investigated. For this purpose, a mixture of ammonia or a control sample (without ammonia) and silver/hydroxide was added to a mixture of AuNRs/ascorbic acid and UV-Vis spectra were recorded. As Fig. 4d shows, the formation of the core/shell nanorods is completed within the first few seconds. Therefore, in all subsequent experiments, spectra were recorded 30 seconds after complete mixing of the sensor components to ensure repeatability of the sensor reaction.

3.3. Figures of merit

The developed probe was tested under optimal conditions to determine its response to different concentrations of ammonia. Fig. 5a shows that as the ammonia concentration increases, the
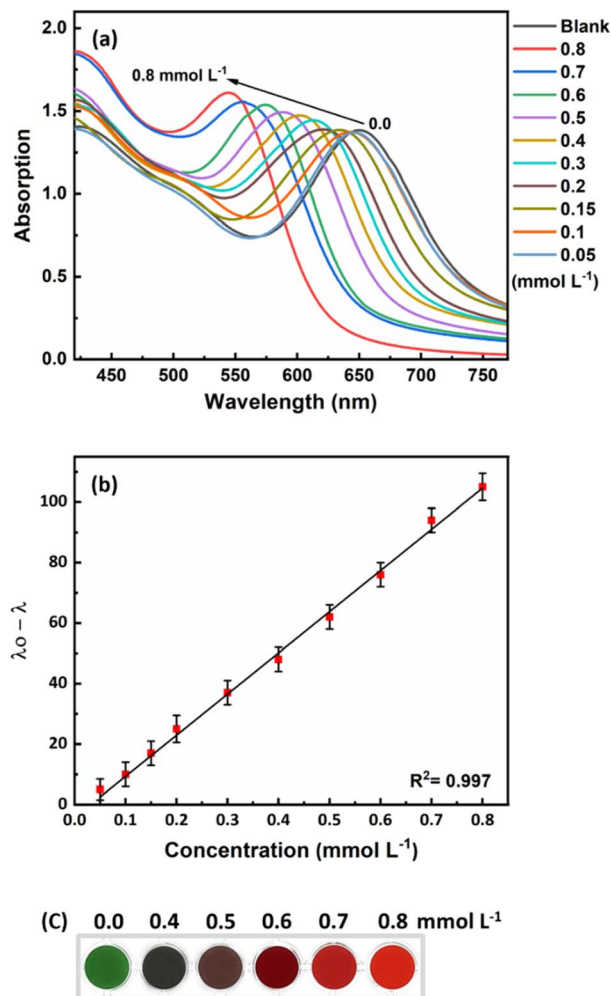
Fig. 5 (a) UV-Vis spectra of the designed probe in the presence of various concentration of ammonia. (b) Plot of sensor's response as a function of ammonia concentrations from 0.05–0.8 mmol L^{-1} (50–800 μmol L^{-1}). (c) Photos of the sensor upon the addition of ammonia. Photos were taken from the top of a 96-well microplate.
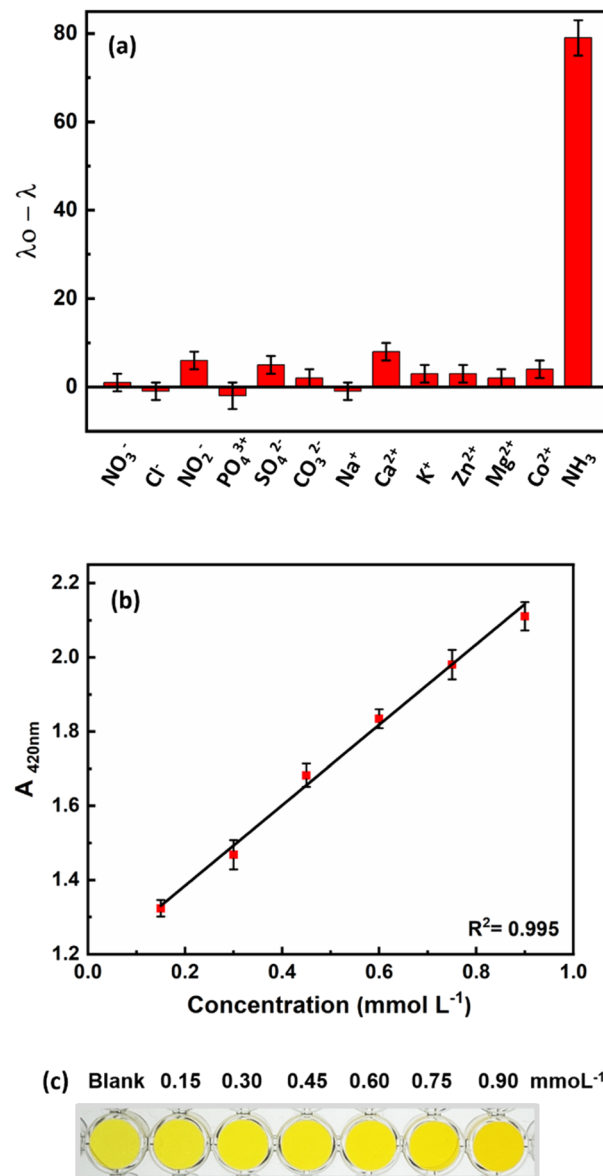

Fig. 6 (a) Selectivity study of designed sensor. (b) The linear relationship between the responses of the Nessler sensor (as standard method) and ammonia concentration. (c) The color change of the Nessler sensor in the presence of different concentrations of ammonia.

longitudinal plasmon peak shifts to shorter wavelengths. The response of the sensor was linear in the range of 50 to 800 μmol L^{-1} (0.85–13.6 ppm) with a detection limit of 44 μmol L^{-1} (0.75 ppm). The calibration curve generated had a suitable R^2 value of 0.997 (Fig. 5b). As the ammonia concentration changed, the color of the sensor solution changed from green to red-orange, which is an excellent detection method for rapid and on-site measurement of ammonia (Fig. 5c).

3.4. Assessment of matrix effect

To determine the selectivity of the proposed method for measuring ammonia in fish culture ponds, some common ions in the culture water environment that may be present in addition to ammonia were investigated under the optimal conditions of this method. The reaction of ions such as NO_3^-, Cl^-, NO_2^-, PO_4^{3+}, SO_4^{2-}, CO_3^{2-}, Na^+, Ca^{2+}, K^+, Zn^{2+}, Mg^{2+}, and Co^{2+} was investigated at a concentration of 25 mmol L^{-1} under optimal conditions. The results (Fig. 6a) show that the proposed

method has a high selectivity for ammonia, despite the possible presence of these ions.

Ammonia concentration is one of the most important parameters to control in water. Given the expansion of the aquaculture industry and the potential negative impact of ammonia on economic development and human health, as well as its ability to harm aquatic animals and damage farming communities, the accurate measurement and control of ammonia levels in fish farm waters is critical. To ensure sustainable use of water resources and to protect aquatic life from the harmful effects of ammonia, it is also crucial to detect and monitor ammonia levels in various water bodies such as breeding ponds. Therefore, the practicality of the developed

Table 1 Detection of ammonia in different real samples by the designed sensor in this work and the Nessler method

Sample	Initial concentration (mmol L^{-1})	Spiked (mmol L^{-1})	Method	Found (mmol L^{-1})	Recovery (%)
Tap water	0.0	0.6	This work	0.591	98.5
			Nessler	0.629	104.8
Campus water	0.0	0.6	This work	0.587	97.8
			Nessler	0.615	102.5
Pond water (sturgeon)	0.033	0.6	This work	0.576	90.5
			Nessler	0.636	100.5
Inlet water (sturgeon)	0.017	0.6	This work	0.588	95.2
			Nessler	0.573	92.7
Pond water (rainbow trout)	0.007	0.6	This work	0.583	96.0
			Nessler	0.624	102.8
Pond water (rainbow trout)	0.010	0.6	This work	0.621	101.8
			Nessler	0.623	102.2
Pond water (rainbow trout)	0.021	0.6	This work	0.587	94.3
			Nessler	0.607	97.7
Pond water (tilapia)	0.031	0.6	This work	0.612	96.8
			Nessler	0.614	97.2

probe was evaluated by detecting ammonia in various water samples, such as tap water, campus water and water from fish breeding ponds. The developed probe was used to test samples spiked with 0.6 mmol L^{-1} ammonia. The results summarized in Table 1 show the feasibility of the developed probe for the determination of ammonia in different samples. In addition, the results are comparable with the standard spectroscopic method according to Nessler. The calibration curve with the Nessler method and the colors of the sensor are shown in Fig. 6b. The Nessler method uses mercury, which is a toxic substance for animals, humans and the environment. However, we used non-toxic, unmodified AuNRs and a growth mechanism that enables colorimetric responses for rapid ammonia detection with the naked eye.

3.5. Comparison with other studies

There are several methods for analyzing ammonia, including amperometry, high performance liquid chromatography (HPLC), thin layer chromatography (TLC), gas chromatography (GC) and conductivity calculations. However, these methods have some limitations, such as slow processing times, high operating temperatures, and specialized expensive equipment requirements.[1] Among these methods, spectroscopic strategies are simpler and cheaper, especially when plasmonic nanoparticles are part of the sensor.

Spectrophotometric methods based on plasmonic nanoparticles that have been reported for the measurement of ammonia are listed in Table 2. The detection limit of ammonia in the present study is lower than the reported methods.[1,31–34,36–39] Most reports do not provide visual detection[1,30,34,36,39] or clear color differentiation.[35,38] In the present study, the color changes of the sensor in the absence and presence of different ammonia concentrations are completely different and can be easily detected by the naked eye. In addition, some of the reported methods require the functionalization of nanoparticles, which makes the fabrication process of the sensor more complicated and time-consuming. However, in the current research, there is no need to modify or functionalize the surface of the nanoparticles. Moreover, some reports are based on specific fruits and plants,[31,33,36] which are only cultivated in a few countries. Therefore, they are expensive and not available.[40]

Table 2 Spectroscopic methods based on plasmonic nanoparticles for ammonia detection

Nanoprobe	LOD (ppm)	Linear range (ppm)	Response time	Ref.
Poly(amidoamine)-coated superparamagnetic iron oxide NPs decorated with AgNPs	5.69	10–50	2 h	30
AgNPs synthesized by Durian fruit shell	—	500–3000	3.5 h	31
AgNPs synthesized by 3-(1-(2-(2,4-dinitrop henyl)hyd razono)ethyl)-1H-indole	17	8–200	30 s	1
AgNPs synthesized by cyanobacterium *Haloleptolyngbya alcalis*	—	50–500	—	32
AgNPs synthesized by fruit extract of *Terminalia chebula*	—	5–100	15 min	33
Core–shell amino-terminated hyperbranched chitosan NPs-AgNPs	8.0	10–50	—	34
Au@Ag NPs	0.11	0.85–27.2	12 min	35
AgNPs synthesized by *Durenta erecta* fruit extract NPs	0.5	5–100	—	36
AgNPs synthesized by poly(methacrylic acid) (PMA)	—	5–100	—	37
AgNPs synthesized by polyvinylpyrrolidone	180	200–1000	20 s	38
AuNRs	0.75	0.85–13.6	30 s	This work

4. Conclusions

In aquaculture, ammonia is a significant pollutant due to its continuous release during the biological processes of aquatic animals. The accumulation of ammonia in water can have negative effects on the environment, including eutrophication and death of aquatic organisms. Therefore, there is an urgent need for accurate, rapid, on-site and sensitive ammonia determination, especially in fish farming systems.[30] In this study, a colorimetric sensor was developed based on the specific dissolution of silver(I) oxide by ammonia, which triggers the activation of silver ions and the subsequent formation of core/shell gold/silver NRs. This led to changes in the surface composition, size, and aspect ratio of the AuNRs, which were accompanied by vivid color changes in the solution from light green to red/orange. Factors affecting the performance of the sensor, such as reducing agent (AA) concentration, silver ion concentration, inhibitory compound (hydroxide ion), pH and reaction time were investigated and optimized to achieve the highest sensitivity in measuring the analyte. The linear range of the sensor was 50–800 μmol L^{-1} with a detection limit of 44 μmol L^{-1}. The effectiveness of this method was confirmed by good results in the measurement of ammonia in tap water, rainbow trout, tilapia, and sturgeon pond farmed water, demonstrating the applicability of this method in real samples. Compared to other ammonia measurement methods, the developed sensor has advantages such as simplicity, low cost, and short analysis time. It also offers acceptable sensitivity and selectivity. Besides all the advantages of the present sensor, its application in seawater samples with high salinity can be challenging. In the case of such samples, a preparation step is needed to remove extra salts from the sample.

Data availability

All data that support the findings of this study are included within the article.

Author contributions

Elahe Ghorbanian: investigation, formal analysis, writing – original draft; Forough Ghasemi: conceptualization, project administration, methodology, writing – original draft; Kamran Rezaei Tavabe: resources, writing – review & editing; Hamid Reza Alizadeh Sabet: resources, validation.

Conflicts of interest

The authors declare no competing interests.

Acknowledgements

References

1 R. G. Elsharkawy and A. A. Ghoneim, *J. Phys. Org. Chem.*, 2021, **34**, e4205.
2 J. H. Tidwell and L. A. Bright, *Encyclopedia of Ecology*, 2018, 91–96.
3 A. G. Leal-Junior, A. Frizera and C. Marques, *Remote Sens.*, 2020, **12**, 1439.
4 I. Zamora-Garcia, F. E. Correa-Tome, U. H. Hernandez-Belmonte, V. Ayala-Ramirez and J.-P. Ramirez-Paredes, *Comput. Electron. Agric.*, 2021, **181**, 105960.
5 P. Soler, M. Faria, C. Barata, E. García-Galea, B. Lorente and D. Vinyoles, *PLoS One*, 2021, **16**, e0243404.
6 L. G. Obeti, J. Wanyama, N. Banadda, A. Candia, S. Onep, R. Walozi and A. Ebic, *J. Environ. Sci. Eng. B*, 2019, **8**, 205.
7 C. Hadfield and L. Clayton, Water quality, *Clinical Guide to Fish Medicine*, 2021, pp. 35–48.
8 A. G. Leal-Junior, A. Frizera and C. Marques, *IEEE Photonics Technol. Lett.*, 2020, **32**, 863–866.
9 D. Li, X. Xu, Z. Li, T. Wang and C. Wang, *TrAC, Trends Anal. Chem.*, 2020, **127**, 115890.
10 S. K. Kailasa, J. R. Koduru, M. L. Desai, T. J. Park, R. K. Singhal and H. Basu, *TrAC, Trends Anal. Chem.*, 2018, **105**, 106–120.
11 P. K. Jain, X. Huang, I. H. El-Sayed and M. A. El-Sayed, *Acc. Chem. Res.*, 2008, **41**, 1578–1586.
12 M. Sepahvand, F. Ghasemi and H. M. S. Hosseini, *Food Chem. Toxicol.*, 2021, **149**, 112025.
13 L. M. Liz-Marzán, C. J. Murphy and J. Wang, *Chem. Soc. Rev.*, 2014, **43**, 3820–3822.
14 F. Ghasemi, A. Naseri and M. Sepahvand, in *Encyclopedia of Green Materials*, Springer, 2022, pp. 1–10.
15 N. Motl, A. Smith, C. DeSantis and S. Skrabalak, *Chem. Soc. Rev.*, 2014, **43**, 3823–3834.
16 C.-C. Chang, C.-P. Chen, T.-H. Wu, C.-H. Yang, C.-W. Lin and C.-Y. Chen, *Nanomaterials*, 2019, **9**, 861.
17 M. R. Mirghafouri, S. Abbasi-Moayed, F. Ghasemi and M. R. Hormozi-Nezhad, *Anal. Methods*, 2020, **12**, 5877–5884.
18 Z. Taefi, F. Ghasemi and M. R. Hormozi-Nezhad, *Spectrochim. Acta, Part A*, 2020, **228**, 117803.
19 A. Mohammadi, F. Ghasemi and M. R. Hormozi-Nezhad, *IEEE Sens. J.*, 2017, **17**, 6044–6049.
20 M. Koushkestani, S. Abbasi-Moayed, F. Ghasemi, V. Mahdavi and M. R. Hormozi-Nezhad, *Food Chem. Toxicol.*, 2021, **151**, 112109.
21 F. Ghasemi, N. Fahimi-Kashani, A. Bigdeli, A. H. Alshatteri, S. Abbasi-Moayed, S. H. Al-Jaf, M. Y. Merry, K. M. Omer and M. R. Hormozi-Nezhad, *Anal. Chim. Acta*, 2023, **1238**, 340640.
22 M. Sepahvand, F. Ghasemi and H. M. Hosseini, *ChemistrySelect*, 2022, **7**, e202103094.
23 H. Rao, X. Xue, H. Wang and Z. Xue, *J. Mater. Chem. C*, 2019, **7**, 4610–4621.
24 M. Sepahvand, F. Ghasemi and H. M. S. Hosseini, *Anal. Methods*, 2021, **13**, 4370–4378.

25 A. Orouji, S. Abbasi-Moayed, F. Ghasemi and M. R. Hormozi-Nezhad, *Sens. Actuators, B*, 2022, **358**, 131479.

26 A. Orouji, F. Ghasemi and M. R. Hormozi-Nezhad, *Anal. Chem.*, 2023, **95**, 10110–10118.

27 Z. Zhang, H. Wang, Z. Chen, X. Wang, J. Choo and L. Chen, *Biosens. Bioelectron.*, 2018, **114**, 52–65.

28 A. Naseri and F. Ghasemi, *Nanotechnology*, 2021, **33**, 075501.

29 L. Scarabelli, M. Grzelczak and L. M. Liz-Marzán, *Chem. Mater.*, 2013, **25**, 4232–4238.

30 O. A. Abdelaziz, R. M. Abdallah, R. A. Khater, A. S. Abo Dena and I. M. El-Sherbiny, *Plasmonics*, 2022, 1–12.

31 E. Alzahrani, *J. Chem.*, 2020, **2020**, 1–11.

32 A. K. Tomer, T. Rahi, D. K. Neelam and P. K. Dadheech, *Int. Microbiol.*, 2019, **22**, 49–58.

33 T. N. J. I. Edison, R. Atchudan and Y. R. Lee, *J. Cluster Sci.*, 2016, **27**, 683–690.

34 I. M. El-Sherbiny, A. Hefnawy and E. Salih, *Int. J. Biol. Macromol.*, 2016, **86**, 782–788.

35 Z. Qiu, Y. Xue, J. Li, Y. Zhang, X. Liang, C. Wen, H. Gong and J. Zeng, *Chin. Chem. Lett.*, 2021, **32**, 2807–2811.

36 M. Ismail, M. Khan, K. Akhtar, M. A. Khan, A. M. Asiri and S. B. Khan, *Phys. E*, 2018, **103**, 367–376.

37 S. T. Dubas and V. Pimpan, *Talanta*, 2008, **76**, 29–33.

38 A. Amirjani and D. H. Fatmehsari, *Talanta*, 2018, **176**, 242–246.

39 S. Pandey, G. K. Goswami and K. K. Nanda, *Int. J. Biol. Macromol.*, 2012, **51**, 583–589.

40 N. A. A Aziz and A. M. Mhd Jalil, *Foods*, 2019, **8**, 96.